A New Test Rig to Study Rolling Element Bearing Thermomechanical Behavior

D. Niel, C. Changenet, F. Ville and M. Octrue

Introduction

The rolling element bearing (REB) is an essential component in mechanical transmission to reduce friction between rotating parts. Now, with the development of the electrical motor in mechanical industry, REBs may work at very high-rotation speed. It leads to an increase of REB power losses and temperatures. In literature several approaches are used to estimate the REB thermomechanical behavior. Hence, for some applications, several divergent viewpoints can be found on thermal behavior modeling according to the dissipation sources taken into account. In order to overcome these discrepancies, a specific test rig was designed to obtain information on REB thermomechanical behavior. This test rig allows for obtaining REB power losses thanks to torque measurement. To study high-speed applications, the ($N.{}_{dm}$) product expected volume is higher than one million.

Nomenclature

d_m	Bearing mean diameter [m]
F	Load [N]
f_0, f_1	Harris model factors [–]
G_{sl}, G_{rr}, K_z	SKF model factors[–]
M	Friction torque [$N.\ mm$]
M_1	Friction torque due to applied load [$N.\ mm$]
M_c	Viscous friction torque [$N.\ mm$]
M_{rr}	Rolling frictional moment [$N.\ mm$]
M_{sl}	Sliding frictional moment [$N.\ mm$]
M_{drag}	Drag frictional moment [$N.\ mm$]
N	Rotational speed [rpm]
R_s	SKF model factor [–]
T	Temperature [°C]
ϕ_{ish}	Inlet shear heating reduction factor [–]
ϕ_{rs}	Kinematic replenishment/starvation reduction factor [–]
μ_{sl}	SKF model factor [–]

Rolling element bearings are widely used in mechanical transmission to reduce friction between two rotating parts. With the further development of the electrical motor in mechanical industry, REBs operate more and more at high rotational speed. For these applications, REBs power losses can be predominant in mechanical transmissions. Several global models can estimate the REB resistive torque (Refs. 1–2). Hence, for some applications, several divergent viewpoints can be found between these models.

In order to overcome these discrepancies, some measurements are required. In the literature, several tests rigs are presented to measure REB torque loss.

A first set of test rigs measure torque loss on REB outer ring. In this case, the REB outer ring has to be mounted in the inner ring of a hydrostatic bearing. The torque is measured via a load sensor located on a beam between the REB outer ring and hydrostatic bearing housing (Ref. 3).

Brecher et al. (Ref. 4) used a hydrostatic bearing to measure the REB torque loss for high-speed application. In this test rig a telemetry system is used to measure the REB inner ring temperature.

Neurouth et al. (Ref. 5) have also used this design to measure the REB frictional torque for grease-lubricated thrust ball bearings.

However the hydrostatic bearing can be complex to use and modifies the outer ring thermal behavior.

REB torque loss can also be measured with strain gauges located on the housing. Hannon (Ref. 6) developed a test rig for four types of REBs within a similar size range. A slip ring allows measuring the REB inner ring temperature. In this test rig, four identical REBs are mounted on the main shaft. The global torque loss is divided by four in order to obtain the REB torque loss. The REBs' torque loss is measured thanks to a strain gauged torque table. This test rig has been developed for low-rotational speed and strong radial load conditions (up to 260 kN).

Pinel et al. (Refs. 7–8) developed a test rig for a 35 mm bore diameter angular-contact ball bearing under thrust load and for very high-speed application; the maximum rotational speed is equal to 72,000 rpm, which corresponds to a ($N.{}_{dm}$) product equals to 3.4 million. The REB torque is measured with strain gauges located near the end of an arm that prevents the housing from rotation. However, this measurement can be complex to realize.

Finally, REB torque loss can be measured on the inner ring by using a torquemeter. In this case, the torquemeter measures the global torque of the shaft. However, some components can affect this measurement (seals, REBs mounting, etc.).

Takabi et al. (Ref. 9) designed an REB test rig to study the deep-groove thermal behavior in oil bath lubrication. The test rig is composed of two REB mountings and one test bearing. A torque sensor measures the torque loss of the system.

REB tests rigs with vertical shaft are also presented in the literature. These test rigs allow testing thrust ball bearings (Ref. 10) or cylindrical (Ref. 11) and tapered roller bearings (Refs. 12–13) under axial load. The torque measurement is realized with a torquemeter located on the vertical shaft.

To finish, some test rigs have been realized only for one application. Ke et al *(Ref.* 14) developed a specific REB test rig

This paper was presented at the 2018 Lyon International Gear Conference and his republished here with permission of the Conference and the authors.

to study the thermal characteristics of double-row tapered roller bearings of a high-speed locomotive. Blake and Truman (Ref. 15) designed a test rig to measure the running torque of tapered roller bearings.

The abovementioned test rigs are dedicated to one operating condition or one size of REB. The new test rig developed in this study is dedicated to a wide range of REB dimensions and for different operating conditions.

In the first section of this paper a new REB test rig design is presented. The second part of this paper is dedicated to the first experimental results.

The New Test Rig Design

Specifications of this test rig. The new test rig has been designed to be able to study the thermomechanical behavior of several kinds of REBs and for different lubrication conditions (grease, oil bath and oil jet). This modularity has been a key point during the test rig design. The tested REB outer diameter is between 72 mm and 150 mm. A lot of REBs can be tested in this test rig: deep groove ball bearings, angular contact ball bearings, roller bearings, etc. Radial and axial load can be applied on the tested REB.

Test rig operation. Thus far, several tests rigs have been presented. For each test rig, a specific method is used to measure the REB torque loss. In this new test rig, REB torque loss measurement is divided into two steps:

- ***Calibration phase*:** Four identical REBs are mounted and work in the same operating condition (rotational speed, radial load, lubrication). These REBs are jet-lubricated with the same lubricant at a given oil injection temperature. The torque loss is divided by four in order to isolate the torque loss of one REB.
- ***Measure phase***: Two REBs (calibration block) are removed and replaced by the tested REB (Fig. 2). The torque loss of mounting blocks (determined in calibration phase) is subtracted to the global torque measurement in order to isolate the contribution of the tested REB.

This architecture requires a specific test rig design. The main challenge is to connect the blocks while maintaining a correct concentricity of the main shaft. Labyrinth seals are used to guarantee oil tightness and to limit power losses. Deep grove ball bearings are used in in the mounting blocks; their characteristics are presented in Table 1; they have been chosen in order to work at high-rotational speed.

Test rig components:

REB lubrication. The REB test rig is composed of two oil tanks. The first one is dedicated to the lubrication of calibration and mounting blocks. These REBs are always lubricated with the same oil at the same temperature (around 70°C). The lubricant properties are presented in Table 2.

The second reservoir is dedicated to the tested REB; it allows testing different lubricants. Gear pumps impose an oil flow between 0 and 1.5 L/min on the REB. Each oil tank is surrounded by hot plates to warm the lubricant. The oil pipes are thermally isolated to reduce heat exchange with the ambient air, allowing for an oil injection temperature even higher than 100°C. The electro spindle maximum rotational speed is equal to 18,000 rpm. A hydraulic jack allows applying a radial load on REB up to 20 kN.

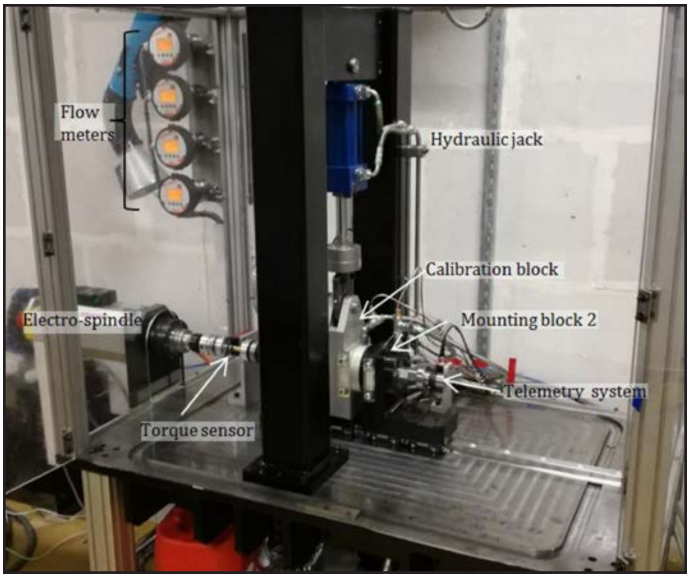

Figure 1 REB test rig.

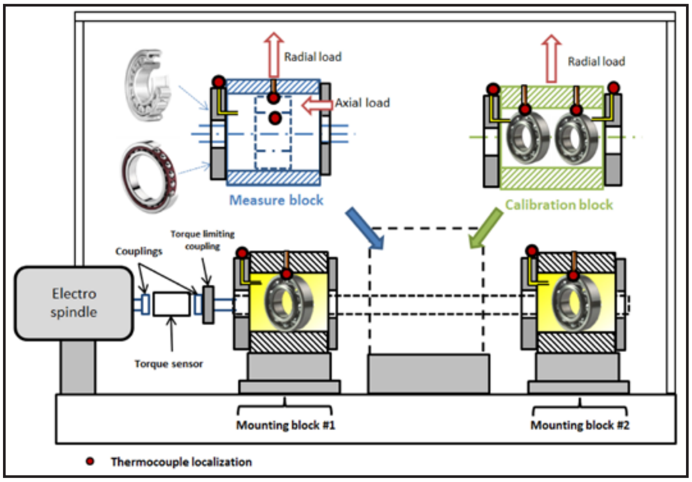

Figure 2 Test rig operation.

Table 1 Main features of the REB used in mounting blocks (SKF 61910)

Designation	Value
Bore dimeter [mm]	72
Outer diameter [mm]	50
Width [mm]	12
Static load [kN]	11.8
Number of balls [-]	16

Table 2 Oil properties

Temperature [°C]	Kinematic viscosity [mm2/s]	density [kg/m3]
20	83.58	864.6
40	36.61	851.6
80	11.67	825.6
100	7.787	[-]

Instrumentation. The test rig instrumentation is presented (Fig. 3). During a test, all the measures are monitored.

A torque sensor (manner 70234) is located on the main shaft between the motor and the mounting block #1. This sensor measures the global torque loss in a range from 0 up to 10 N.m. A torque limiter protects the sensor when the torque loss is up to the maximum value. Type-T thermocouples are located on the fixed and rotating parts of the blocks. For all REBs the outer ring temperature is measured to prevent unusual overheating. The oil inlet and outlet temperatures are measured to study oil heat transfer inside the REB. As ambient air has an influence on the test rig's thermal behavior, this temperature is also measured. On the tested REB, the inner ring and shaft temperatures are measured. A telemetry system located on the tip of the shaft allows transmitting temperatures to the data acquisition card. The force sensor (SCAIME K1427) is located on the extended piston rod of the hydraulic cylinder; this sensor measures the applied load. Flow sensors (Kobold ZOK-ExK/ZxK) are located upstream of each oil injection circuit.

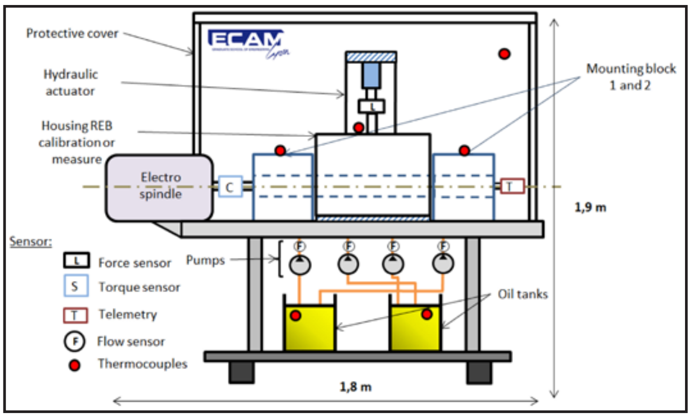

Figure 3 Test rig instrumentation.

Table 3 Mounting block REB operating condition

Designation	Value
Rotational speed	[0–12,300] rpm
Oil flow	12 L/h
Oil injection temperature	70°C
Radial load	400N or 1.2 kN
Axial load	0N

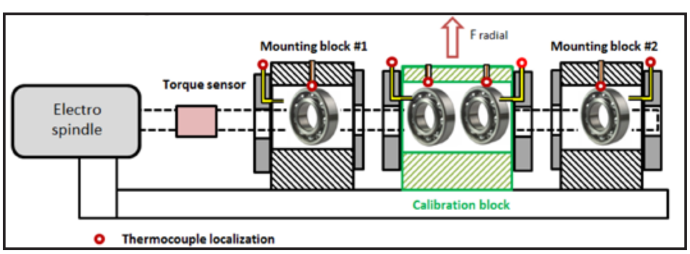

Figure 4 Calibration phase.

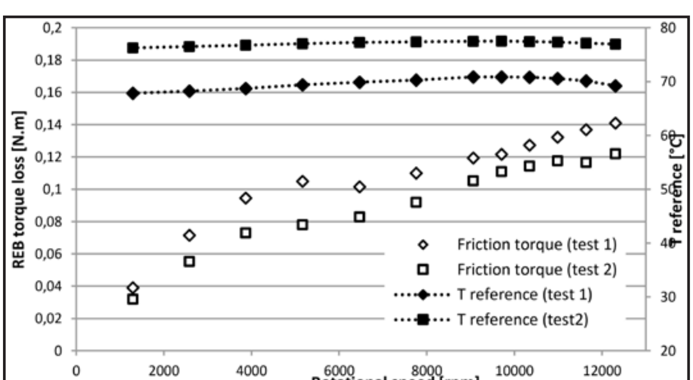

Figure 5 Mounting block REB friction torque (radial load 400N).

Mounting blocks characterization. The first test is dedicated to characterize the dissipation of the mounting blocks; to do that, the operating conditions are presented (Table 3). The oil flow in a REB is constant during the test for the entire rotational speed range. As presented previously, in the calibration phase four identical REBs are mounted on the main shaft. The global torque that is measured can be divided by four in order to isolate the torque loss of one REB.

In order to take into account the influence of REB thermal behavior on its frictional torque, a temperature of reference is defined in Equation 1.

$$T_{ref} = \frac{T_{outer\ ring} + T_{oil\ injection}}{2} \quad (1)$$

During testing, the bulk temperature of a REB can evolve with the test rig thermal behavior (ambient air temperature, oil inside the tank, etc.). In order to take this phenomenon into account, several tests have been carried out for different oil injection temperatures. Figure 5 shows the mounting block REB friction torque for two different temperatures. Figure 5 also underlines that reference temperature increase leads to a torque loss diminution. This experimental result is consistent with global power losses models. The same tests have been realized for a radial load equal to 1.2 kN. Thanks to this approach, the mounting blocks' torque loss can be estimated as a function of its thermal behavior.

Experimental Results and Discussion

This second part is dedicated to the first experimental results obtained on the new test rig. In order to analyze these results, the measured torque loss is compared with some calculated values.

REB torque loss global models. In the literature several models are used to estimate REB torque loss. Global models provide a torque loss value with limited numbers of input data.

Harris model. To estimate power loss dissipation in REB, Harris developed an empirical power loss model (Ref. 2). The torque loss for one REB (M_{harris}) is divided into two contributions — M_l is the friction torque due to the applied load and M_c the viscous friction torque.

Where M_l is defined by

$$M_l = f_1 F_{dm} \times 103 \quad (2)$$

And M_c is defined by

$$\upsilon \cdot N < 2000 \qquad M_c = 160 \times 10^{-7} \cdot f_o \cdot (d_m \times 10^3)^3 \quad (3)$$

$$2000 < \upsilon \cdot N \qquad M_c = 10^{-7} \cdot f_o \cdot (\upsilon N)^{2/3} \cdot (d_m \times 10^3)^3 \quad (4)$$

This model is developed for REB of mean diameter d_m under a static equivalent load F and at a rotational speed N. The factor f_1 depends on the bearing design and load, and f_o depends on the kind of REB and lubrication.

SKF model. To calculate REB power losses, SKF Company has also developed a global model (Ref. 1); this model is derived from computational models. The friction torque can be estimated by the following equation:

$$M_{SKF} = M_{rr} + M_{sl} + M_{drag} \tag{5}$$

The rolling frictional moment M_{rr} is defined by:

$$M_{rr} = \phi_{ish}\,\phi_{rs}\,G_{rr}\,(\upsilon N)^{0.6} \tag{6}$$

Where ϕ_{ish} is the inlet shear heating reduction factor and ϕ_{rs} is the kinematic replenishment/starvation reduction factor. The number G_{rr} depends on the kind of REB, its design and load.

The sliding frictional moment is determined by:

$$M_{sl} = G_{sl} \cdot \mu_{sl} \tag{7}$$

Where G_{sl} depends on the kind of REB, its design, and load. The sliding friction coefficient μ_{sl} depends on the lubricant shearing and for boundary lubrication on asperity contacts.

The frictional moment of drag losses for ball bearing is defined by:

$$M_{drag} = 0.4 \cdot V_m \cdot K_z \cdot (d_m \times 10^3)^5 \cdot N^2 + 1{,}093 \cdot 10^{-7} \cdot N^2 \cdot (d_m \times 10^3)^3 \left(\frac{N \cdot (d_m \times 10^3)^3 \cdot f_t}{\upsilon}\right)^{1.379} \cdot R_s \tag{8}$$

Where parameters V_m, K_z, f_t and R_s depend on the REB geometry.

Tested REB measurement. In the measure phase, two REBs located in the calibration block are replaced by the tested REB (Fig. 6).

The torque loss generated by mounting blocks can be estimated thanks to the experimental results obtained in the calibration phase (Fig. 5). During a test, oil inlet, oil outlet, inner and outer ring temperatures are measured. The first tested REB is a deep groove ball bearing. Its main features are presented in Table 4.

A test is divided into several steps. First of all, the test rig works at low rotational speed (about 5,000 rpm) to warm up the blocks. Hot plates located around the oil tanks warm up the lubricant until the oil injection temperature is around 70°C. The requested oil flow and radial load are applied on the tested REB. Progressively, the rotational speed is increased from 5,000 rpm to the maximum rotational speed range. When the measured torque loss value is stabilized, the test can begin.

First results and discussion. The results presented here are given for a radial load applied on the tested REB, which is equal to 400N. As far as the lubrication conditions are concerned, the oil flow is equal to 25 L/h and the oil injection temperature is around 70°C. These experimental results are compared with numerical results obtained through the abovementioned global models.

In Figure 7, torque loss calculated with Harris model is compared with experimental results. To perform this comparison, in Equation 4 the coefficient f_0 is set to 2 and the lubricant viscosity is calculated at outer ring temperature. Torque loss calculated thanks to global models are in the same order of magnitude as the measured torque loss. However, global models do not taken into account the REB torque loss variations.

Figure 7 underlines that torque loss evolution according to the rotational speed can be divided into 3 zones: from 0 to about 5,000 rpm the torque loss value increases with the rotational speed. In this zone, the resistive torque can be accurately estimated by using the Harris model. Then, from 5,000–10,000 rpm, the torque loss value appears to be almost constant; both models do not take into account this torque loss stabilization in their calculations. Last but not the least, from 10,000–12,300 rpm the torque loss evolution has a steep increase with the rotational speed. These increases begin when the ($N.{}_{dm}$) product is around 0.85 million. For both models, REB torque loss is not well estimated. The Harris model underestimates the REB torque loss. At the opposite, the SKF model overestimates the REB torque loss. This overestimation has already been observed in another study (Ref. 16). Finally, this increase for high-speed application is probably due to drag loss (Ref. 17).

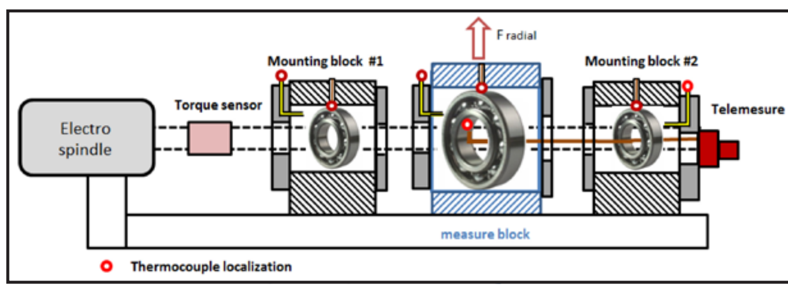

Figure 6 Measure phase.

Table 4 Main features of the tested REB (reference SKF 61815)	
Designation	**Value**
Bore diameter (mm)	75
Outer diameter (mm)	95
Width (mm)	12
Static load (kN)	14.3
Number of balls (-)	26

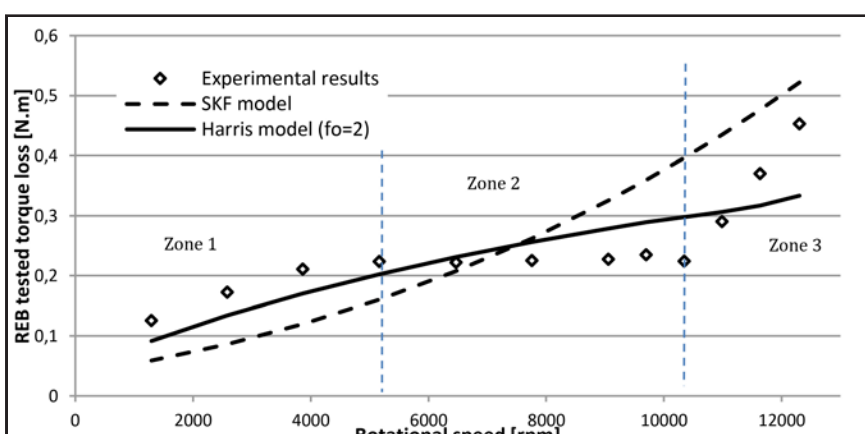

Figure 7 REB tested torque loss and global models (radial load 400N, oil injection temperature 70°C, oil flow 25 L/h).

For zone 1 and 2, it is interesting to note that the modified SKF model can provide good torque loss estimation. In this case radial and axial load have to be equal to 10 percent of the REB tested static load.

In Figure 8, torque loss calculated with SKF model, the load radial load is equal to 10 percent of the REB tested static load. The viscosity is also calculated at the outer ring temperature. Figure 8 underlines that REB torque is well estimated in zone 1 and 2 by using a SKF model without drag loss. But in zone 3, no model can correctly estimate the REB torque loss.

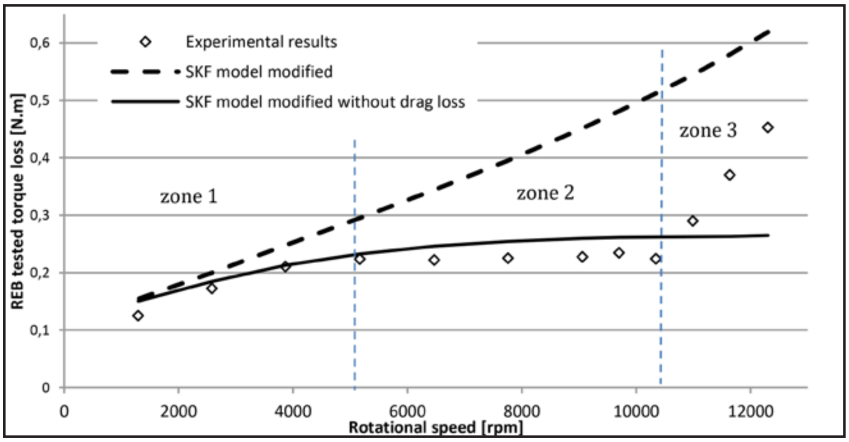

Figure 8 REB tested torque loss and SKF model modified (radial load 400N oil injection temperature 70°C oil flow 25 L/h).

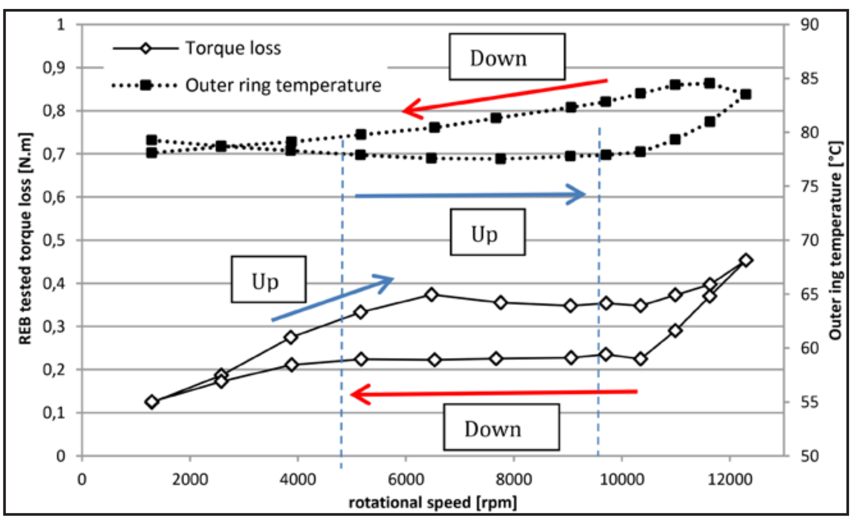

Figure 9 Influence of the rotational speed and REB outer ring temperature on the torque loss (test at 400N, oil injection temperature 70°C, oil flow 25 L/h).

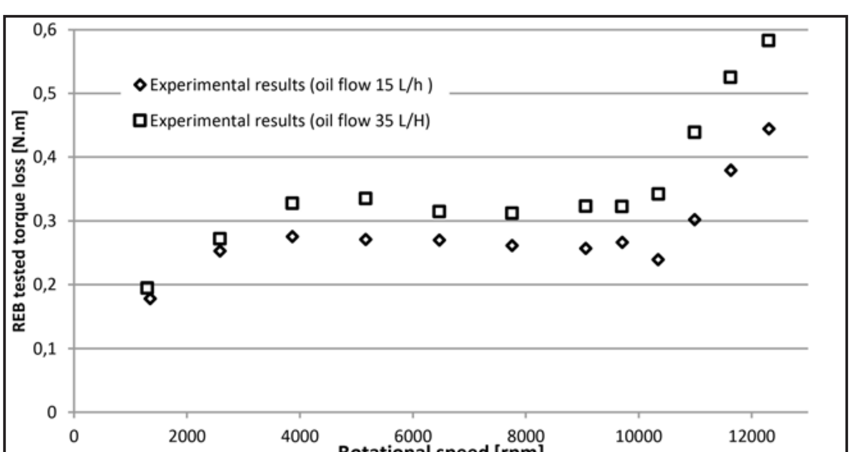

Figure 10 Influence of the oil flow on the torque loss (oil injection temperature 50°C, load 400N).

Influence of the operating condition on the REB torque loss. In this section the influence of the oil flow and REB thermal behavior on the torque loss are studied.

REB thermal behavior influence on the torque loss. Figure 9 shows the REB torque loss and its outer ring temperature according to the rotational speed. At the beginning of the test, the tested REB operates at a rotational speed equal to 1,300 rpm and under a radial load of 400N. The oil flow is equal to 25 L/h with an inlet temperature about 70°C. These operating conditions are constant during the entire test. The rotational speed is gradually increased from 1,230 rpm to 12,300 rpm. Then the rotational speed is gradually decreased. The torque loss evolution is similar to the one observed in the previous section. During the first phase (rotational speed increase), the outer ring temperature is constant in zones 1 and 2. In zone 3 the torque loss rise leads to a REB outer ring temperature increase.

During the down phase (rotational speed decrease), the torque loss evolution is similar to the one obtained during the first phase. But, as the REB is hotter, its torque loss is smaller — especially in zone 2.

To conclude, Figure 9 underlines that the REB thermal behavior has a huge impact on the REB torque loss.

Influence of oil flow. In order to study the impact of the oil flow on REB torque loss, several tests have been carried out for different oil flows at a given oil injection temperature (equal to 50°C), and under a radial load of 0.4 kN.

Figure 10 underlines that, for high-speed application, the oil flow has a predominant impact on the frictional torque. For instance, at 12,300 rpm an oil flow increase of 15 L/h leads to a rise of about 20% in REB frictional torque. Moreover, it can be noted that oil flow modifies the REB thermal behavior, and thus affects its frictional torque. This parameter is not taken into account in global models and it could be interesting to take it into account.

Conclusion

This research work aims to present a new REB test rig dedicated to the study of the thermomechanical behavior of this mechanical component.

In the first part of this paper, this new test rig is presented. It has been designed to study different kinds of REBs and for different operating conditions.

The second part is dedicated to the first results that have been obtained. An 85 mm pitch diameter deep groove ball bearing was tested under different operating conditions. Experimental results have been compared with global models of power losses. This part underlines that these models can estimate the REB torque loss for low-speed application. However, when the ($N._{dm}$) product tends toward a million, the REB torque loss increases suddenly; this increase is not correctly taken into account in the global models. Moreover, the influence of the REB thermal behavior and the oil flow rate on the REB torque loss were highlighted. **PTE**

Acknowledgement. *The authors would like to thank M. Vincent Ricol and DRA Company for their relevant work during the test rig design.*

Funding. *The authors would like to thank the Cetim, the ANRT CIFRE n°2015/0809 and the Carnot Institute Ingénierie@Lyon for the support and the funding.*

Dr. Dimitri Niel is a graduate of the ECAM Lyon (Masters' Degree in mechanical engineering) in 2015. He received his PhD in 2018 in Mecanical Engineering at INSA Lyon (LaMCoS), ECAM Lyon (LabECAM) and Cetim; his thesis was on thermos-mechanical behavior of high-speed rolling element bearings. Niels research focus is thermos-mechanical behavior of rolling element bearing, test rig design and experimental bearings testing.

Prof. Christophe Changenet has since 1992 been a researcher and lecturer at ECAM Lyon (Ecole Catholique d'Arts et Metiers de Lyon) — the institution's graduate school of engineering. From 1998 until 2008, he was head of the Department of Mechanical Engineering and Energetics at ECAM Lyon and, since 2008, Changenet has served as the school's head of research.

Prof. Fabrice Ville is a professor and researcher at INSA Lyon, where he is a member of the Mechanical Systems and Contacts research group.

Dr. Michel Octrue is employed at CETIM (an Academic member of AGMA), French Technical Center, dedicated to mechanical industries in the field of mechanical power transmission as a specialist in the behavior of mechanical components (gears, roller bearings, etc.). His expertise is focused on projects involving mechanical power transmission components and their integrations in gear reducers, machines, and systems for automotive and transportation devices. His experience covers the different stages — from the design-calculation, choice of tolerances, selection of materials and heat treatment, development and validation by numerical simulation, but also gear measurement and testing. He is also focused on design, project management and analysis (fatigue, failure analysis) in testing engineering for mechanical power transmission components. Octrue is also closely involved with the Technical Committee for French Gear Manufacturers at CETIM and in the development of gear standards with AFNOR, UNM and ISO, e.g. — he is convenor of ISO TC60/SC1/WG7 on worm gears. Octrue retired from CENTIM in 2018 but continues to serve there in a consultant capacity.

References

1. SKF Group. *Rolling bearings 6000 EN.* Göeteborg, Sweden: SKF Group 2013.
2. T. A. Harris, *Rolling Bearing Analysis*, 4th Ed., New York, United States of America: John Wiley& Sons, 2001.
3. A. Neurouth, C. Changenet, F. Ville, and A. Arnaudon, "Thermal modeling of a grease lubricated thrust ball bearing," vol. 228, no. 11, pp. 1266–1275, 2014.
4. B. W. WZLl, R. Aachen, O. S. Gmbh, and G. Corresponding, "High- Speed Rolling Bearing Test Rigs with Contactless Signal Transmission for Measuring the Inner Ring Temperature," *European Telemetry and Test Conference 2014*, pp. 116–121.
5. A. Neurouth, C. Changenet, F. Ville, and A. Arnaudon, "Thermal modeling of a grease lubricated thrust ball bearing," *STLE 2014 Orlando*, vol. 228, no. 11, pp. 1266–1275, 2014.
6. W. M. Hannon, T. A. Barr, and S. T. Froelich, "Rolling-Element Bearing Heat Transfer — Part III : Experimental Validation," *J. Tribol. ASME*, vol. 137, pp. 1–13, 2015.
7. I. Pinel, H. R. Signer, S. Technical, and V. Zaretsky, "Design and Operating Characteristics of High-Speed , Bearings."
8. S. H. R. Schuller F. T. , Pinel S.I., "Operating characteristics of a high speed, jet lubricated 35 millimeter bore ball bearing with a single outer land guided cage," *NASA Tech. Pap.* April, 1980.
9. J. Takabi and M. M. Khonsari, "On the thermally induced failure of rolling element bearings," *Tribol. Int.*, Vol. 94, pp. 661–674, 2016.
10. C. M. C. G. Fernandes, R. C. Martins, and J. H. O. Seabra, "Tribology International Friction torque of thrust ball bearings lubricated with wind turbine gear oils," *Tribiology Int.*, Vol. 58, pp. 47–54, 2013.
11. S. J. Fernandes CM, Amaro PM, Martins RC, "Torque loss in cylindrical roller thrust bearings lubricated with wind turbine gear oils at constant temperature," *Tribiology Int.*, Vol. 67, pp. 72–80, 2013.
12. J. Liebrecht, X. Si, B. Sauer, and H. Schwarze, "Investigation of Drag and Churning Losses on Tapered Roller Bearings," *J. Mech. Eng.*, Vol. 61, no. 6, pp. 399–408, 2015.
13. V. Paleu and D. Nelias, "On Kerosene lubrication of hybrid ball bearings," *Int. Conf. diagnosis Predict. Mech. Eng. Syst.*, Vol. 2007, No. Xiii, pp. 50–56, 2007.
14. Y. Ke, W. Ning, Z. Qiang, Zh. Yongsheng, Z. Jinhua, and N. Qingbo, "Theoretical and experimental investigation on the thermal characteristics of double-row tapered roller bearings of high speed locomotive," *Int. J. Heat Mass Transf.*, Vol. 84, pp. 1119–1130, 2015.
15. J. J. Blake and C. E. Truman, "Measurement of running torque of tapered roller bearings," *Pro. IMechE, Part J J. Eng. Tribol* vol. 218(4) pp. 239–249, 2004.
16. D. Niel, C. Changenet, F. Ville, and M. Octrue, "Thermomecanical study of high speed rolling element bearing : A simplified approach," *Pro. IMechE, Part J J. Eng. Tribol* vol. 0, no. 0, pp. 1–12, 2017.
17. F. Pouly, C. Changenet, F. Ville, P. Velex, B. Damiens, U. De Lyon, E. Lyon, and L. Energétique, "Investigations on the power losses and thermal behavior of rolling element bearings," *Pro. IMechE, Part J J. Eng. Tribo.*, Vol 224(9) pp. 925–933, 2009.

For more information.

Have questions or comments regarding this technical paper? Contact Dimitri Niel at *dimitri.niel@ecam.fr*.